Desalination and Water Treatment
www.deswater.com

doi:10.5004/dwt.2016.1728

59 (2017) 230–242
January

Application of response surface methodology for modeling and optimization of malachite green adsorption by modified sphagnum peat moss as a low cost biosorbent

Farimah Sarbisheh, Reza Norouzbeigi*, Farnaz Hemmati, Hadi Shayesteh

School of Chemical Engineering, Iran University of Science & Technology (IUST), Narmak, Tehran, Iran, email: farimah_sarbisheh@chemeng.iust.ac.ir (F. Sarbisheh), Tel. +98 21 77240495; Fax +98 21 77240495; email: norouzbeigi@iust.ac.ir (R. Norouzbeigi), email: farnaz_hemmati@chemeng.iust.ac.ir (F. Hemmati), email: hadi_shayesteh@chemeng.iust.ac.ir, hadi.shayesteh91@gmail.com (H. Shayesteh)

Received 10 December 2015; Accepted 1 July 2016

ABSTRACT

This study focused on the adsorption of malachite green (MG) using hydrochloric acid modified sphagnum peat moss (SPM) from aqueous solution. A response surface method (RSM) based on the Box–Behnken design (BBD) was used to determine the effects of initial dye concentration (20–60 mg L^{-1}), adsorbent dosage (0.6–1.6 g L^{-1}) and pH of the solution (2.5–6.5). Characterization of the SPM has been accomplished by SEM, BET, and FTIR analysis. Based on the obtained equilibrium time (90 min), in each initial MG concentration, adsorption kinetics was better described by the pseudo-second order kinetic model and the results showed that the adsorption isotherm data were fitted well to the Langmuir isotherm. Calculate values of the statistical parameters such as R^2, R^2_{adj}, and R^2_{pred}, were 0.9946, 0.9850 and 0.9144, respectively. Applying the method of the desirability function, optimization of SPM dosage (0.6 g L^{-1}), initial MG concentration (60 mg L^{-1}) and pH (6.43) gave a maximum adsoption uptake of 93.71 mg g^{-1} with desirability of 1.000 by the modified SPM. Regeneration ratio of SPM was also investigated for the removal of MG.

Keywords: Sphagnum peat moss; Malachite green; Box-Behnken design; Adsorption; Optimization

1. Introduction

In recent years, removal of synthetic dyes from industrial effluents (textile, food technology, hair colorings and so on) has become one of the most serious environmental problems in many countries. These colors and dyes discharge large amount of pollutions into the water, whereas most of them are mutagenic, carcinogenic and toxic compounds. The presence of these materials in water and environment could directly adverse effects on our life [1–4]. MG is a cationic triarylmethane dye which is widely consumed for coloring foodstuffs, industrial and analysis applications [5,6]. Furthermore, MG is applied in various industries such as aquaculture as agent to treat parasiticide, fungal and bacterial infections [3]. Despite its widely usages, many of dyes such as MG due to mutagenic, carcinogenic and teratogenic properties would cause various health problems in the living environment of humans and animals [7,8]. Therefore, the colored industrial effluent has to be properly treated before it is discarded into the environment.

Nowadays, in addition to techniques such as precipitation [9], cloud point extraction [10,11], ion exchange [12], ultrafiltration [13], coagulation [14] and flocculation [15], adsorption process has been recognized as an attractive, popular, efficient and superior separation method for the uptake of dyes and wide range of compounds from wastewater because of its flexibility, simplicity and effectiveness [16–18].

In recent years, there are demands for low-cost materials for the removal of pollutants such as dyes and ions from wastewater [19,20]. Hence, adsorbents such as clays [21], sawdust [22], red mud [4], zeolite [23], nanoparticles [8, 24], *Hibiscus cannabinus* fiber [25] and agricultural wastes [26] have been used for dye removal from aqueous solu-

*Corresponding author.

tions. Sphagnum peat moss (SPM) is a low cost biomaterial that showing a good ability in the treatment of wastewater [27,28]. Peat moss mainly consists of lignin, cellulose and humic materials [29]. SPM is widely used as an adsorbent for removal of dyes and other contaminants from aqueous solutions [28,30,31]. It has light brown with large specific surface area and highly porous structure (95%) [28,32]. Peats are inexpensive and easily available natural materials that widely available in many countries. Peats, as an adsorbent, have high cation exchange capacities and excellent ion-exchange properties [33,34]. Therefore, peat was chosen as the study material.

In statistics science, design of experiments (DOE) is widely applied for modeling and optimizing process parameters [35]. Conventionally, the classical method of experimental (one factor at a time optimization approach) involves the effect of independent variable at a time while maintaining others different variables at a fixed level, which is a complex method, extremely time consuming, expensive for a large number of variables and often leads to mistake to results when interactions between different variables are present. For this reason RSM commonly used for optimization of widely various processes [36–39]. RSM is an empirical mathematical and statistical technique used to establish significant relationships between set of controllable experimental factors with one or more dependent variables by carrying out a limited number of experiments [37,39,40]. Among the various methods of RSM, central composite design (CCD) and Box-Behnken design (BBD) are commonly used for the response optimization. These two designs are such methods which are based on the three and five levels incomplete factorial designs, respectively [38]. Compared to the CCD method with the same number of factors, BBD requires fewer experiments and this technique is considered as the most suitable for evaluating quadratic response in cases [37]. In the BBD, the number of runs needed for the development of BBD is defined as $N = 2k\ (k + 1) + \theta_\circ$, where N, k and $\theta_\circ$ are the number of experiments, factor number and replicate number of the central point, respectively [36].

The aim of the present study is to investigate the influence of several parameters such as adsorbent dosage, solution pH and the initial dye concentration on the MG removal from aqueous solution using acid modified SPM using BBD. The three factors BBD were selected for modeling and optimizing the adsorption conditions and the adsorption capacity was selected as the response of the experiments. Also, the kinetics, isotherms, and contact time studies were also performed. As we know there is not any report on the empirical modeling of the MG removal by the modified SPM.

2. Materials and methods

2.1. Materials

MG, analytical grade ($C_{23}H_{25}ClN_2$, Mw = 364.92 g mol^{-1}, color index 42000, λ_{max} = 617 nm) was purchased from Merck (Merck Co., Germany) and used without further purification. Chemical structure of MG is shown in Fig. 1. Irish sphagnum peat moss was supplied from Shamrock

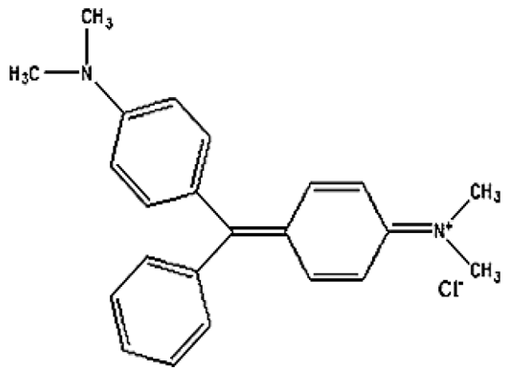

Fig. 1. Chemical structure of MG.

Company (Ireland). Two times distilled water was used for solution preparation and the initial pH was adjusted using 0.5 N HCl (Merck) or 0.5 N NaOH (98%, Merck) solutions.

2.2. Preparation of the acid modified adsorbent

The SPM used was washed several times using distilled water to remove the primary impurities and all the dirt particles. The washed SPM was dried at ambient temperature for 24 h. Then, it was crushed and sieved with mesh size #60 to achieve particle size about 300 μm. Then, 20 g of SPM was poured into a beaker containing boiling water and stirred for 90 min. Then samples were put in boiling 1 N HCl solution for 60 min to complete the modification of the adsorbent. To remove additional HCl at the surface, SPMs were washed with distilled water. At the end, the solution was filtered with Whatman filter papers (No. 3) and SPMs were dried at ambient temperature for 24 h. The prepared adsorbent was kept in an isolated container.

2.3. Characterization of the adsorbent

Fourier transform infrared spectroscopy study was carried out at wavelengths in the range 450–4000 cm^{-1} (Perkin Elmer Spectrum, RX1, Germany) to analyze the functional groups, using potassium bromide (KBr) pressed disk technique. The adsorbent morphology was investigated by VEGA\\TESCAN scanning electron microscope (SEM) operating at 30 kV accelerated voltage. Besides, the specific surface area was measured by a NOVA® Station B Surface Area Analyzer using N_2 sorption method and the Brunauer–Emmett–Teller (BET) model.

2.4. Adsorption studies

This research was divided into two parts; the first study was the evaluation of the contact time using 0.6 g L^{-1} of adsorbent, and 250 mL of various initial MG concentrations (20, 40, 60 mg L^{-1}) at the pH of 6.5. The second step was the selection of a three levels, three factors BBD to investigate the adsorption capacity. For this purpose, a stock solution (200 mg L^{-1}) was prepared by dissolving proper amount of MG in deionized water and different concentrations of dye

solutions were prepared by this solution. The adsorption process was carried out in a batch system at room temperature. In each experiment, after adjusting the solution pH (PL-250, EZODO, Taiwan), required amount of adsorbent was added to the 250 mL of different initial MG concentrations. Then, the solution was agitated at 160 rpm. At the equilibrium state the suspensions were filtered using filter paper (No. 3). The residual concentrations of MG in the supernatants were analyzed using a double beam UV–visible spectrophotometer (Shimadzu UV-1800, Japan) at λ_{max} = 617 nm.

The amount of dye adsorbed per unit mass of the adsorbent as well defined by the adsorption capacity, q_e (mg g^{-1}), was calculated using Eq. (1):

$$q_e = (C_0 - C_e)\frac{V}{M} \tag{1}$$

where C_o and C_e are the initial and equilibrium concentrations of the MG (mg L^{-1}) respectively, V is the volume of the batch solution (L), and M is the amount of the adsorbent (g) used in the experiments.

2.5. Box-Behnken experimental design

Box–Behnken experimental design was applied using Design Expert 9.0.4.1 (Stat-Ease, Inc.) to our study with three factors at three levels. The variables under investigation were initial MG concentration (A), SPM dosage (B) and pH of the solution (C) and the response data (Y) was the adsorption capacity of MG onto the SPM. The suitable contact time was achieved 90 min in the first stage and it was kept constant for all experiments. The factor levels were selected based on the preliminary experiments and were coded as –1 (low), 0 (central point or middle) and 1 (high). Experimental variables and their levels of the BBD are given in Table 1.

A total of 15 batch runs have been performed in this work to optimize three main independent parameters on the adsorption capacity (Table 2). For analyzing of the results, a non-linear and second-order regression model was used to describe the effects of the selected factors and factor interaction. Considering all the linear, square and linear by linear interaction items, the quadratic response model can be described as follows (Eq. 2):

$$Y = \beta_0 + \sum_{i=1}^{k}\beta_i x_i + \sum_{i=1}^{k}\beta_{ii}x_i^2 + \sum_{1\le i\le j}^{k}\beta_{ij}x_i x_j + \varepsilon \tag{2}$$

where Y is the predicted response (adsorption capacity); x_i and x_j are coded variables and β_o, β_i, β_j and β_{ij} are the offset term, linear effect of the input factors, quadratic effect of input factor and linear interaction effect between the input factors, respectively [35,41].

Table 1
Experimental range and levels of independent process variables

Variable	Notation	Range and levels		
		Low (–1)	Middle (0)	High (+1)
Initial MG concentration (mg L^{-1})	A	20	40	60
SPM dosage (g L^{-1})	B	0.6	1.1	1.6
pH	C	2.5	4.5	6.5

2.6. Error analysis

The non-linear regression has been an important tool to determine the best model compared to the experimental data. Due to the inherent bias resulting from linearization, three non-linear error functions were applied. The error equations employed were as follows [36]:

Nonlinear chi-square test (χ^2):

$$\chi^2 = \sum_{i=1}^{n}\left[\frac{\left(q_{e,\exp} - q_{e,cak}\right)^2}{q_{e,cak}}\right]_i \tag{3}$$

The average relative error (ARE):

$$ARE = \sum_{i=1}^{n}\left|\frac{\left(q_{e,\exp} - q_{e,cak}\right)}{q_{e,\exp}}\right|_i \tag{4}$$

A derivative of Marquardt's percent standard deviation (MPSD):

$$MPSD = \sum_{i=1}^{n}\left[\left(\frac{q_{e,\exp} - q_{e,cdc}}{q_{e,\exp}}\right)^2\right]_i \tag{5}$$

In the above equations, the subscripts "exp" and "calc" indicate the experimental and calculated values of adsorption capacities, respectively.

3. Results and discussion

3.1. SPM Characterization

FTIR spectroscopy analysis was performed to evaluate the present functional groups on the SPM surface. Related spectrum is illustrated in Fig. 2. The broad absorption bands observed at 1626 and 1052 cm^{-1}, can be related to the characteristic peaks of lignite aromatic C=C and polysaccharides C–O absorption bands, respectively. The peaks observed at 3430, 2924 and 1708 cm^{-1} may be assigned to bending of hydroxyl (–OH), C–H and C=O groups, respectively [42,43].

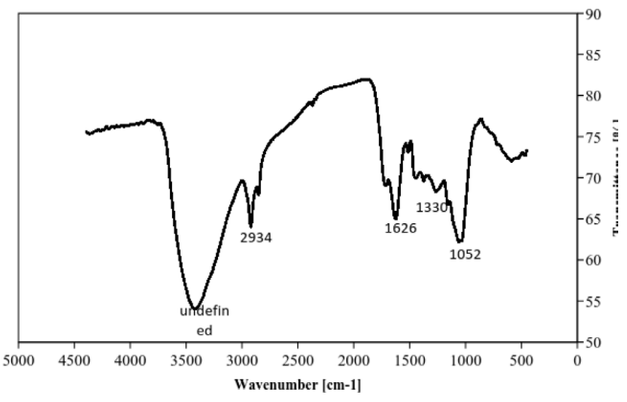

Fig. 2. FTIR spectrum of the SPM.

Table 2
Experimental and predicted values of Y for MG adsorption onto the modified SPM

Run order	Coded values			Levels			Adsorption capacity	
	A	B	C	Initial MG concentration (mg L^{-1})	SPM dosage (g L^{-1})	pH	Experimental value (mg g^{-1})	Predicted value (mg g^{-1})
1	+1	+1	0	60	1.60	4.5	37.3875	35.779
2	–1	0	–1	20	1.10	2.5	17.9306	15.419
3	0	0	0	40	1.10	4.5	36.1299	36.17
4	0	0	0	40	1.10	4.5	36.165	36.17
5	+1	0	+1	60	1.10	6.5	54.1657	56.679
6	0	–1	–1	40	0.60	2.5	57.8835	58.8
7	0	+1	–1	40	1.60	2.5	24.6706	24.88
8	+1	–1	0	60	0.60	4.5	93.102	90.779
9	0	+1	+1	40	1.60	6.5	24.9719	24.06
10	–1	–1	0	20	0.60	4.5	32.9692	34.579
11	0	0	0	40	1.10	4.5	36.2293	36.17
12	–1	+1	0	20	1.60	4.5	12.4679	14.779
13	–1	0	+1	20	1.10	6.5	17.8955	16.499
14	+1	0	–1	60	1.10	2.5	51.0458	52.439
15	0	–1	+1	40	0.60	6.5	65.1457	64.94

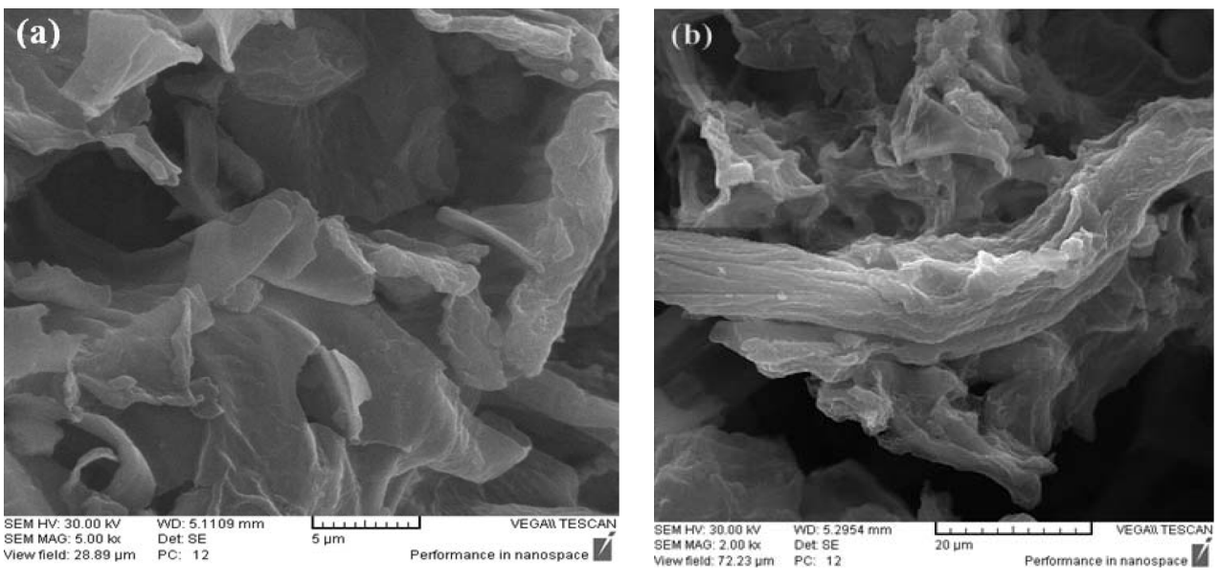

Fig. 3. Scanning electron microscopy (SEM) images of acid treated SPM before adsorption (a) and used biosorbent after MG adsorption (b).

Fig. 3 shows the SEM micrographs of the SPM samples before and after MG adsorption. As it can be seen, SPM has a highly porous, cellular and irregular texture. After adsorption of MG, large area and porous texture of the modified SPM covered with dye molecules which can be seen in Fig. 3b. As well, the surface area of the SPM was estimated by N_2 sorption isotherm using the commonly utilized the Brunauer–Emmett–Teller (BET) model. Accordingly, the specific surface area of the used SPM samples was 150 m^2 g^{-1}. These results indicate that modified SPM is suitable for adsorption because it has large surface area and porous texture.

3.2. Effect of contact time

Contact time is one of the most important parameters in the absorption process. Fig. 4 illustrates the effect of contact

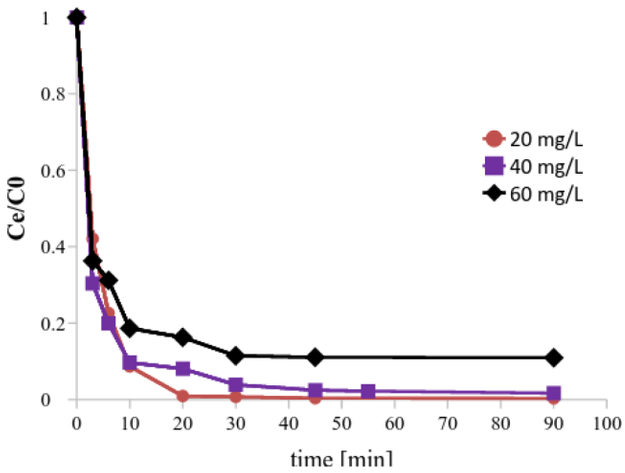

Fig. 4. Effect of contact time on the adsorption capacity of SPM [feed pH of 6.5, SPM dosage 0.6 g L^{-1}, temperature of 20°C and 160 rpm agitation speed].

time on the MG removal at initial MG concentrations of 20, 40 and 60 mg L^{-1}. As it is shown in Fig. 4, the adsorption rate of MG on the SPM would rise sharply for the first 10 min, and after that would become slow up to the 45 min mark. After the 90 min, there was little change in the absorption rate and it reflects that process would reach to the equilibrium state. As a result, to ensure complete equilibrium state, all of the experiments were performed for 90 min. Most of the absorption process consists of two stages; rapid adsorption rate at the initial times and slow absorption rate at the end of the experiment. Rapid adsorption rate at the initial contact time may be referred to the large number readily accessible sites and may be concerned as high affinity of the MG molecules and the SPM surface. As well, the slow absorption rate at the end of the experiment can be due to the saturation of the available adsorbing sites and decreased number of vacant sites of adsorbent [4,15].

3.3. Adsorption kinetics

In order to describe the adsorption kinetics or mechanism for the adsorption of MG dye onto the acid modified SPM, the pseudo-first-order, pseudo-second-order and intra-particle diffusion models were applied to test the experimental data which are shown in linear form by Eqns. (6)–(8), respectively. [4,44].

$$\log(q_e - q_t) = \log q_e - \frac{k_1}{2.303} \tag{6}$$

$$\frac{t}{q_t} = \frac{1}{k_2 q_e^2} + \frac{t}{q_e} \tag{7}$$

$$q_t = k_{id} t^{\frac{1}{2}} + C \tag{8}$$

where q_t (mg g^{-1}) and q_e (mg g^{-1}) are adsorption capacities at time t (min) and the equilibrium condition, respectively; and k_1 (min^{-1}) and k_2 (g mg^{-1} min^{-1}) are the Lagergren rate constant of pseudo-first order and the rate constant of pseudo-second-order model, respectively. C is the constant parameter related to the thickness of the boundary layer (mg g^{-1}) and k_{id} is intra-particle diffusion rate constant (mg g^{-1} $min^{-1/2}$).

For the pseudo-first-order model as it can be observed in Fig. 5a, The pseudo-first-order rate constant (k_1) and the theoretical equilibrium adsorption capacities ($q_{e,cal}$) determined from the intercept and the slop of the linear plot of $\log(q_e - q_t)$ vs. t. The plot of t/q_t vs. t for the linear pseudo-second-order model has been plotted (Fig. 5b) and the pseudo-second-order rate constant (k_2) and theoretical equilibrium adsorption capacities ($q_{e,cal}$) were determined from

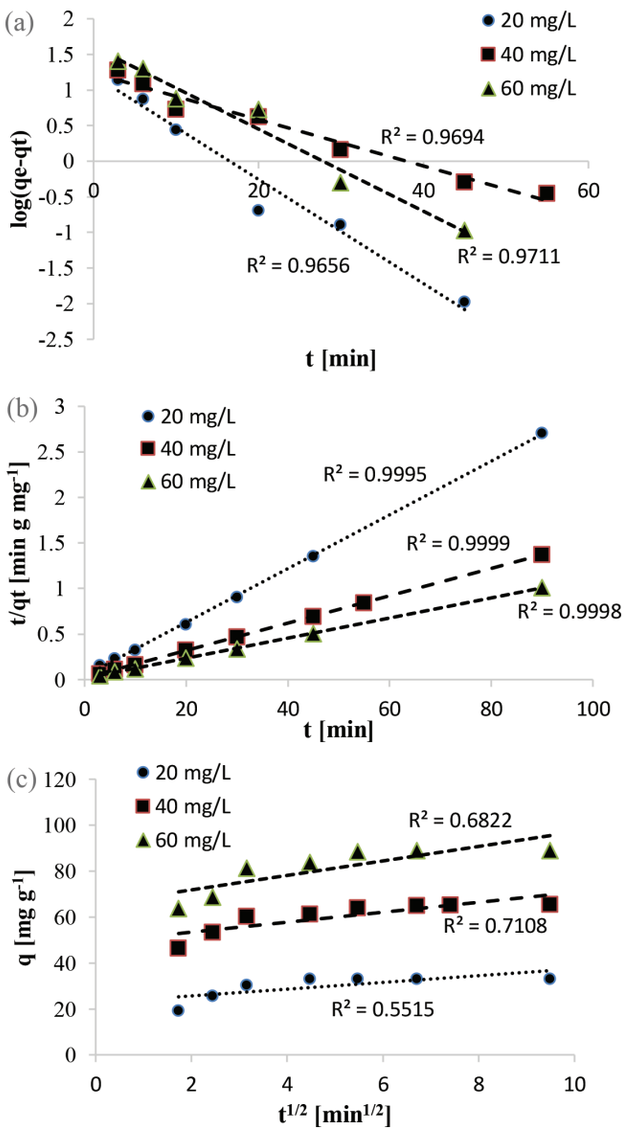

Fig. 5. Adsorption kinetics of MG adsorbed by SPM: (a) pseudo-first-order model, (b) pseudo-second-order model, (c) intra-particle diffusion model.

the intercept and the slope of this linear plot. Finally, C and k_{id} were determined from the intercept and the slope of the plot of q_t versus t (Fig. 5c).

The adsorption kinetics data were evaluated by the aforementioned kinetics models, and calculated parameters are given in Table 3. As a result, the value of correlation coefficient (R^2) obtained from pseudo-second-order kinetics, 0.9995, 0.9999 and 0.9995 for 20, 40, 60 mg L^{-1} initial MG concentrations, respectively, were higher than those obtained for pseudo-first-order kinetics and intra-particle diffusion model. So the pseudo-second-order model could reasonably describe the MG adsorption on the SPM. In addition, for each initial MG concentration the examined adsorption capacity, $q_{e,exp}$, were closer to these which were estimated (calculated) by the pseudo-second order kinetic model ($q_{e,cal}$). Similar results have been reported for the adsorption of MG onto Walnut shell [25], activated sintering process red mud [4] and Durian seed-based activated carbon [45].

3.4. Adsorption equilibrium

In order to describe the adsorption equilibrium for the adsorption the Langmuir, Temkin and Freundlich isotherm models were applied to test the experimental data which are shown in non-linear form by the following equations, respectively [46].

$$q_e = \frac{q_m K_L C_e}{1 + K_L C_e} \tag{9}$$

$$q_e = \left(\frac{RT}{b_T}\right) 1n\left(K_T C_e\right) \tag{10}$$

Table 3
Adsorption kinetic parameters for adsorption of MG onto the SPM

MG concentration (mg L^{-1})			
	20	40	60
Pseudo-first-order			
$q_{e,exp}$ (mg g^{-1})	33.23	65.55	89.04
$q_{e,cal}$ (mg g^{-1})	3.34	3.44	4.97
k_1 (min^{-1})	0.1683	0.0751	0.1329
R^2	0.9656	0.9694	0.9711
Pseudo-second-order			
$q_{e,exp}$ (mg g^{-1})	33.23	65.55	89.04
$q_{e,cal}$ (mg g^{-1})	33.33	66.66	90.91
k_2 (g mg^{-1} min^{-1})	0.1084	0.0114	0.0083
R^2	0.9995	0.9999	0.9998
Intra-particle model			
$q_{e,exp}$ (mg g^{-1})	33.23	65.55	89.04
k_{id} (mg g^{-1} $min^{-1/2}$)	0.4166	2.1687	3.1542
C (mg g^{-1})	30.26	49.06	65.50
R^2	0.5515	0.7108	0.6822

$$q_e = K_F C_e^{1\backslash n} \tag{11}$$

where q_e is the equilibrium amount of adsorbate (mg g^{-1}), q_m is maximum adsorption capacity, (mg g^{-1}) and C_e, K_L are equilibrium concentration of adsorbate (mg L^{-1}) and Langmuir constant (L mg^{-1}) related to the affinity of binding sites and the free energy of sorption, respectively. T, R, b_T and K_T in Temkin isotherm model are the absolute temperature (K), gas universal constant (8.314 J mol^{-1} K), the Temkin constant related to the enthalpy of adsorption (J mol^{-1}) and equilibrium binding constant (L g^{-1}), respectively. K_F (((mg g^{-1})/(mg $L^{-1})^{1/n}$)) and n in Freundlich isotherm are the Freundlich constants. K_F and n values indicated the sorption capacity and the sorption intensity of the system, respectively. For favorable adsorption, the value of the Freundlich constant should be in the range of 1–10. The Langmuir isotherm model is based on the assumption of homogeneous surface of the sorbent, while it is mainly applied to describe the monolayer adsorption process. The Temkin isotherm is also available for the effects of some indirect adsorbate-adsorbate interaction on a surface and the Freundlich isotherm model expressed for adsorption heterogeneous surface and interactions between adsorbed molecules [46].

The adsorption capacity of the SPM with different dye concentrations at equilibrium condition are shown in Fig. 6. According to Fig. 6, the adsorption capacity increased with the increasing initial dye concentration due to that a higher initial concentration could increase the overcoming the resistances to the mass transfer of dye between the solution and solid phases, which the probability of collision enhance between the dye molecules and the adsorbents [46]. It is obvious from Fig. 6 that for SMP Langmuir isotherm fits the adsorption data better than the Freundlich and Temkin isotherms. To better express, the adsorption parameters were evaluated using non-linear forms of the Langmuir, Freundlich and Tempkin isotherm models, the calculated values of these isotherms parameters, and values of different related error analyses are given in Table 4. The goodness of fit criteria for the models may be checked and represented by comparison of the calculated non-linear correlation coefficients (R^2). The high value of the non-linear regression coefficient for the Langmuir isotherm shows that this model give good fit to the adsorption isotherm. In addition, it can be seen from Table 4 that the values of error analyses for the Langmuir are lower than that of the other isotherms, which

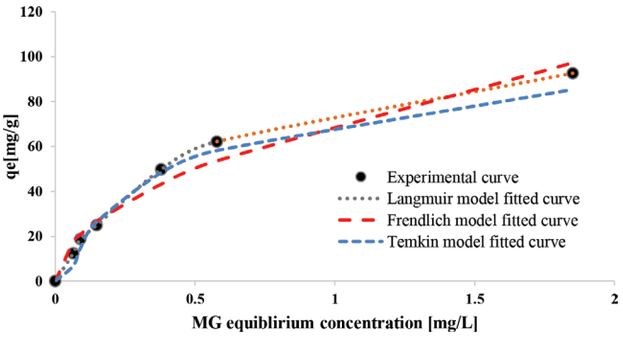

Fig. 6. Adsorption isotherms and fitted curves (non-linear correlation) of MG adsorption onto the SPM.

Table 4.
Adsorption isotherm constants and values of different error analyses for isotherm models (non-linear methods)

Langmuir	
q_m(mg g^{-1})	120.16
K_L(L mg^{-1})	1.8342
R^2	0.9982
χ^2	0.1804
ARE	0.1519
MPSD	0.0092
Freundlich	
K_F (mg g^{-1})(L mg^{-1})$^{1/n}$	70.9287
$1/n$	0.5116
R^2	0.9668
χ^2	4.5790
ARE	0.8943
MPSD	0.2134
Temkin	
b_T(J mol^{-1})	104.4077
K_T (L g^{-1})	20.8713
R^2	0.9913
χ^2	4.3225
ARE	0.8914
MPSD	0.2621

verifies the applicability of the Langmuir and for adsorption of MG onto the SPM. Therefore, the adsorption of MG onto the SPM is considered as monolayer adsorption on a homogeneous surface without interaction between the dye molecules [47,48].

3.5. Adsorption studies using Box-Behnken design

The BBD optimization process involves main steps: (i) conducting designed experiments; (ii) proposing the statistical model using regression analysis technique; (iii) Using diagnostic plots to checking the adequacy of the obtained model and experimental results; (iv) predict the experiment response at a certain factor and level combination and consequently checking model using a confirmation test [37,40].

To estimate the regression coefficient, a multiple regression analysis was performed on the experimental data. Linear, interactive, quadratic and cubic models were fitted to the experimental data to obtain the regression equations. To decide about the adequacy of models among the various models to represent, two different common tests namely sequential model sum of squares and model summary statistics were carried out [37,41,49]. According to Table 5, Cubic model was found to be aliased. Sequential model sum of squares indicate that the *p*-value was lower than 0.01 for quadratic model only. Model summary statistics showed that the excluding cubic model which was aliased, quadratic model was found to have maximum "Adjusted R-Squared" and the "Predicted R-Squared" values. Therefore, quadratic model was chosen for further analysis.

Therefore, after performing experiments according to BBD (Table 2), second-order polynomial (as the model of the experimental design) function of the adsorption capacity with factors interaction terms was obtained (Eq. (12)):

Table 5
Adequacy of the model tested

Source	Sum of squares	df	Mean square	F value	*p*-value	Remark
Sequential model sum of squares						
Mean	23853.02	1	23853.02			
Linear	5793.16	3	1931.05	35.65	< 0.0001	
2FI	324.59	3	108.20	3.19	0.0842	
Quadratic	3	79.04	11.56	11.56	0.0110	Suggested
Cubic	34.19	3	11.40	4491.58	0.0002	Aliased
Residual	5.075E-003	2	2.537E-003			
Total	30242.10	15	2016.14			
Source	Std. Dev.	R-Squared	Adjusted R-Squared	Predicted R-Squared	PRESS	
Model Summary Statistics						
Linear	7.36	0.9067	0.8813	0.8067	1235.32	
2FI	5.82	0.9575	0.9257	0.8007	1273.05	
Quadratic	2.62	0.9946	0.9850	0.9144	547.05	Suggested
Cubic	0.050	1.0000	1.0000		+	Aliased

$$Y_{predicted} = 36.17 + 19.30A - 18.70B + 1.33C - 8.80AB + 0.79AC - 1.74BC - 0.051A^2 + 7.86B^2 - 0.86C^2 \quad (12)$$

where $Y_{predicted}$ is predicted adsorption capacity (mg g^{-1}), and A, B and C are the coded variables corresponding to the initial MG concentration, SPM dosage and pH of the solution, respectively.

Analysis of variance (ANOVA) is a common statistical method that assays the significance and the adequacy of the total variation in a set of data into component parts associated with specific sources of variation for the target of trial hypotheses on the factors of the model [36]. Also, this technique was used to test the statistical significance of the proposed quadratic model. To measure how well the suggested model fits the experimental data, the statistical parameters of F-value, R^2, *p*-value, and lack of fit were evaluated [50]. The ANOVA result is reported in Table 6. From data of Table 6, it can be fined that the model was highly significant at 95% of confidence level for uptake of MG dye using modified SPM due to its *p*-value is lower than 0.0001. Thus, the model can be used to predict the adsorption capacity with Eq. (12). As a general rule, values of *p*-value less than 0.0500 indicate the significant of the source of variation. The F-value of "the lack of fit" term is 0.5461 and it implies that the lack of fit is not significant [51].

The quality of the regression equation was further expressed by the correlation coefficients. R^2, R^2_{adj} and R^2_{pred} are experimental, adjusted and model predicted values, respectively. Fig. 7 shows the relationship between experimental and predicted values from the model calculated by Eq. (12). R^2_{adj} is a modified R^2 that has been adjusted for the number of terms in the model and the proximity of these values indicates that unnecessary variables have not been included [40]. The calculations showed that R^2, R^2_{adj} and R^2_{pred} values were 0.9946, 0.9850 and 0.9144, respectively. The obtained little difference between the values of R^2_{adj}, and R^2_{pred} (0.0706) indicates that there is a good correlation between the model and the experimental data. As a general rule, the difference higher than 0.2 in the values of R^2_{adj}, and R^2_{pred} indicates the disagreement between the experimental data and the fitted model [36].

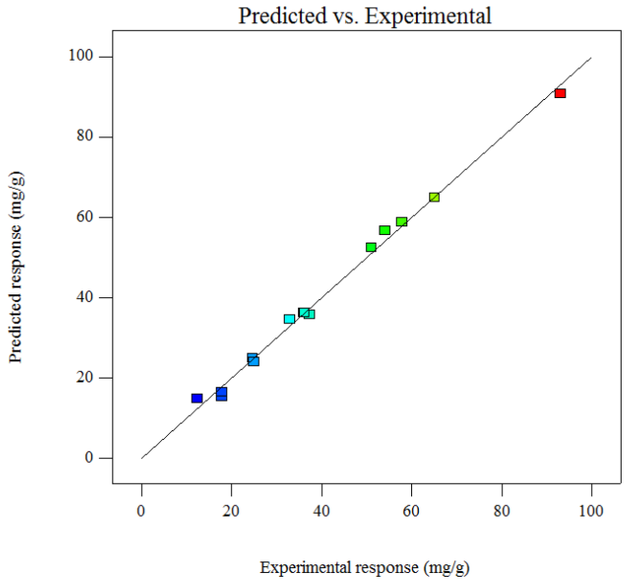

Fig. 7. The actual and predicted response plot of MG adsorption capacity onto the modified SPM.

Based on the ANOVA (Table 6), the P-values were utilized as a tool to introduce the significant or non-significant variables. Each variation source with *p*-value less than 0.05 would be a significant one. Accordingly, the effects of A, B, AB and B^2 are significant, while non-significant variables can be C, AC, A^2, BC and C^2. It implies that the initial MG concentration, SPM dosage, and initial MG concentration

Table 6
Regression analysis for quadratic response surface model fitting (ANOVA)

Source	Sum of squares	df	Mean square	F Value	*p*-value	Remark
Model	6354.88	9	706.10	103.25	< 0.0001	Significant
A-Initial MG Concentration	2981.38	1	2981.38	435.94	< 0.0001	
B-SPM dosage	2797.61	1	2797.61	409.07	< 0.0001	
C-pH	14.17	1	14.17	2.07	0.2095	
AB	309.99	1	309.99	45.33	0.0011	
AC	2.49	1	2.49	0.36	0.5727	
BC	12.11	1	12.11	1.77	0.2407	
A^2	$9.529*10^{-3}$	1	$9.529*10^{-3}$	$1.393*10^{-3}$	0.9717	
B^2	227.98	1	227.98	33.33	0.0022	
C^2	2.76	1	2.76	0.40	0.5532	
Residual	34.20	5	6.84			
Lack of Fit	34.19	3	11.40	1.33	0.5461	non-significant
Pure Error	$5.075*10^{-3}$	2	$2.537*10^{-3}$			
Cor Total	6389.07	14				

and SPM dosage interaction have a significant effects on the adsorption capacity. As it can be find from Table 6, the effects of initial concentration and SPM dosage were highly significant ($p < 0.001$).

After determining the significant factors, statistically insignificant terms ($p > 0.05$) were deleted from the quadratic equation to obtain a modified response surface model (Eq. (13)):

$$Y_{predicted} = 36.17 + 19.30A - 18.70B - 8.80AB + 7.86B^2 \quad (13)$$

Fig. 8a–d show diagnostic plots of this optimization study. Data were also investigated to check the normality of the residuals. The normal probability chart is shown in Fig. 8a for adsorption capacity of MG. According to Fig. 8, almost all points are laid on the diagonal line and closely follow the theoretical distribution. So, the normality was satisfied. Furthermore, the normal distribution (histogram) curve shows no derivation from the normality (Fig. 8b).

Fig. 8c and 8d show the standardized residuals vs. predicted adsorption capacity of SPM. In both graphs, the standardized residuals should oscillate in a random pattern around the center line and should be placed within the interval of ±3.50. The figures show that there is no potential outlier among the experiment outputs [40].

3.6. Interaction effect of adsorption process variables

Fig. 9 shows response surface curves and contour plots for the amount of the adsorption capacity in corresponding interaction effects. The graphical representations were drawn according to the regression analysis and were used to demonstrate the relationship between the adsorption capacity and factors. These plots are useful for investigating the main and interaction effects of the variables [35,51].

Fig. 9a shows the combined effect of the initial MG concentration and SPM dosage on the adsorption capacity. When the SPM dosage is constant and pH value is less than 4.5, the adsorption capacity increases significantly with an increase of initial MG concentration. Mass transfer driving force would increase logically with an increase of the initial dye concentration. However, increasing initial concentra-

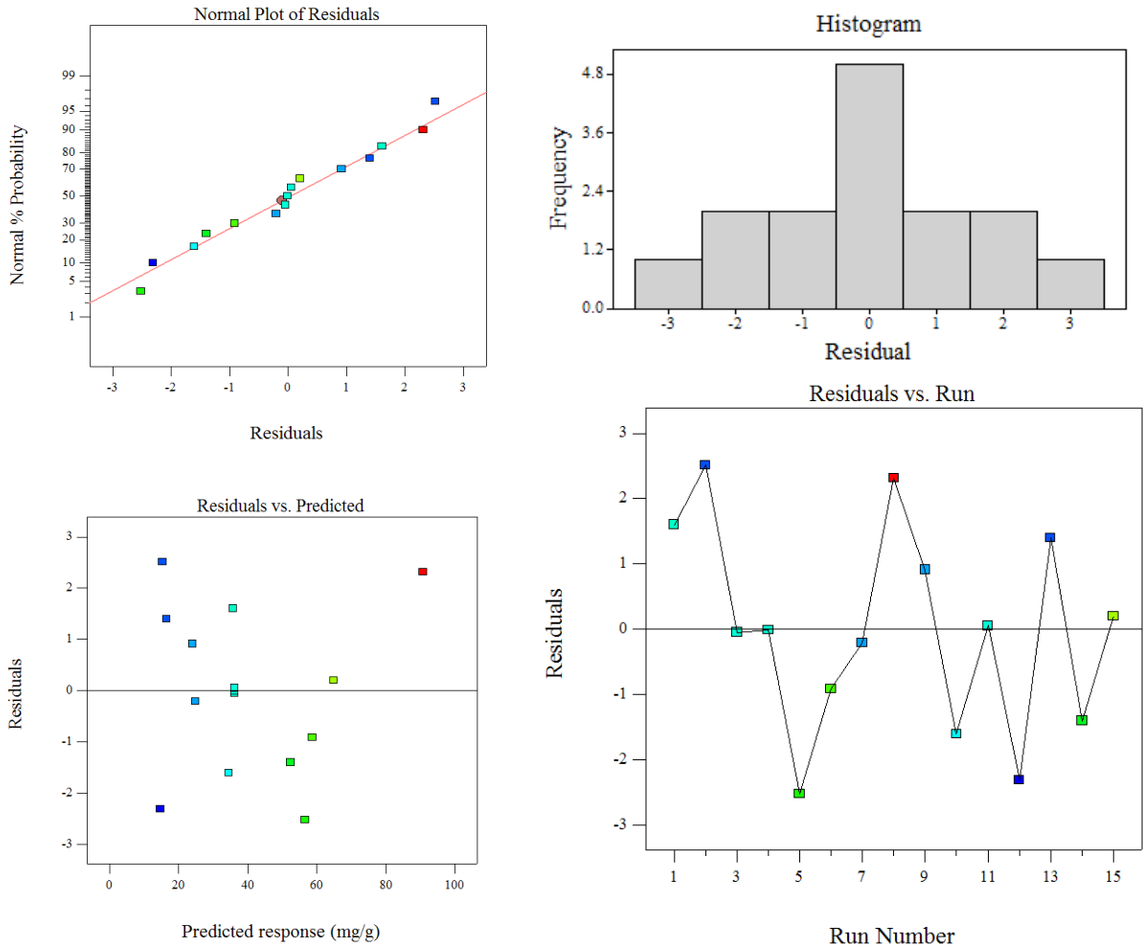

Fig. 8. Standardized residual plots versus (a) normal probability, (b) predicted response , (c) histogram and (d) run number for uptake of MG.

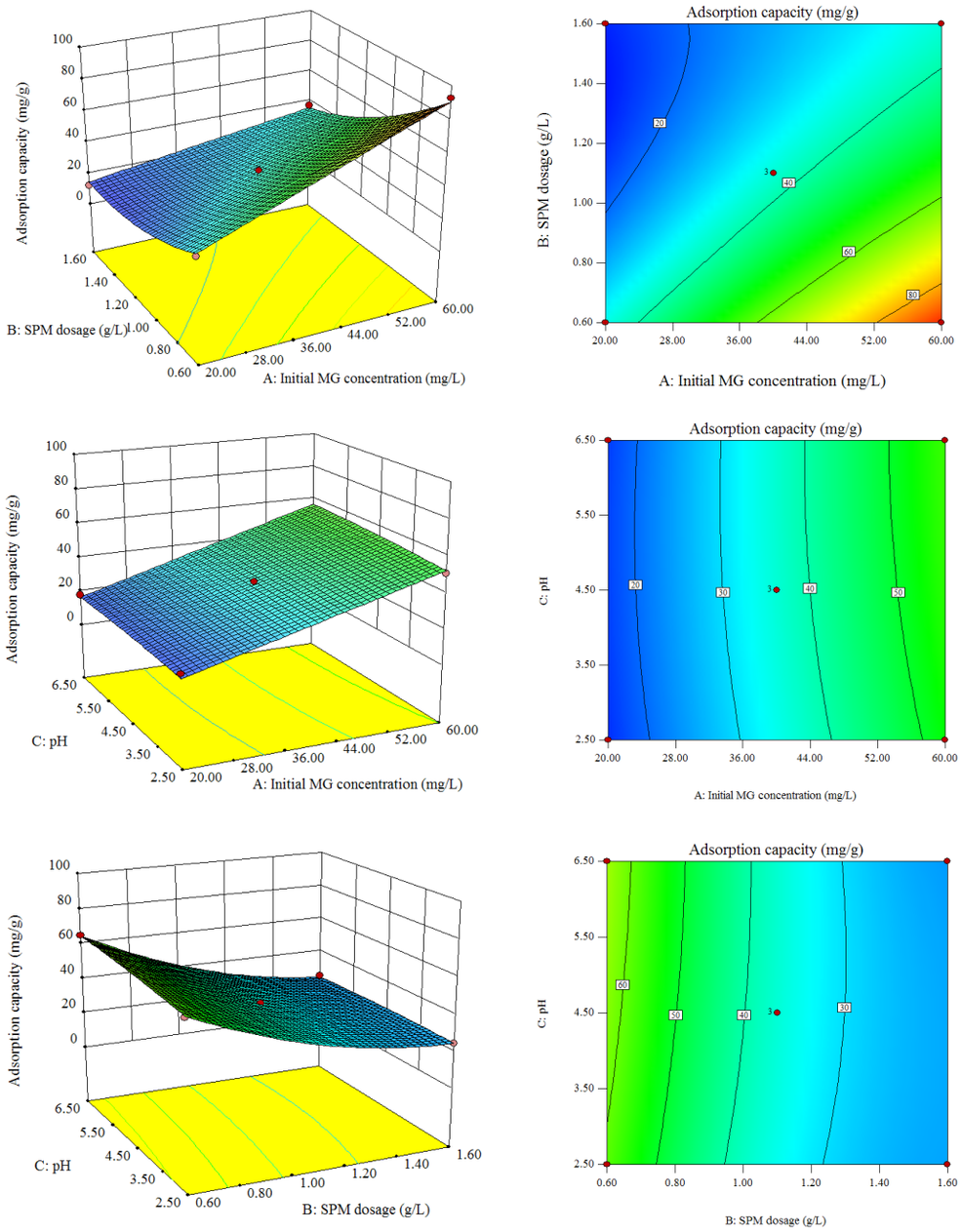

Fig. 9. Response surface plots and contour-line plots of predicted adsorption capacity.

tion enhances the probability of the collision between the MG molecules and the SPM adsorbing sites [47,52]. Similarly, when the initial MG concentration is constant, the adsorption capacity would increase gradually decreasing the SPM dosage. The resulted adsorption capacity decrement can be mainly due the unsaturated sites during the adsorption and therefore, excess amounts of adsorbent would be required for the uptake of dye molecules [47,53]. It could be indicated that the effects of the SPM dosage and the initial MG concentration increasing were negative and positive, respectively, when changing from lower to the higher levels.

From Fig. 9b, c, it can be clearly seen that the pH of the solution had not a significant effect when compared with the initial dye concentration and SPM dosage. Low values of the coefficients in the Eq. (12) such as C, AC, BC and C^2 may be presented as another evidence. The adsorption capacity of the sorbent did not change when the initial MG concentration was constant and the SPM dosage was 1.1 g L^{-1}. Similarly, when the initial MG concentration is 40 mg L^{-1} and the SPM dosage is constant, the adsorption capacity of MG does not change. Respectively, Fig. 9b, c show a significant change of initial MG concentration and SPM dosage when pH of the solution is constant, which these results explained in Fig. 9a.

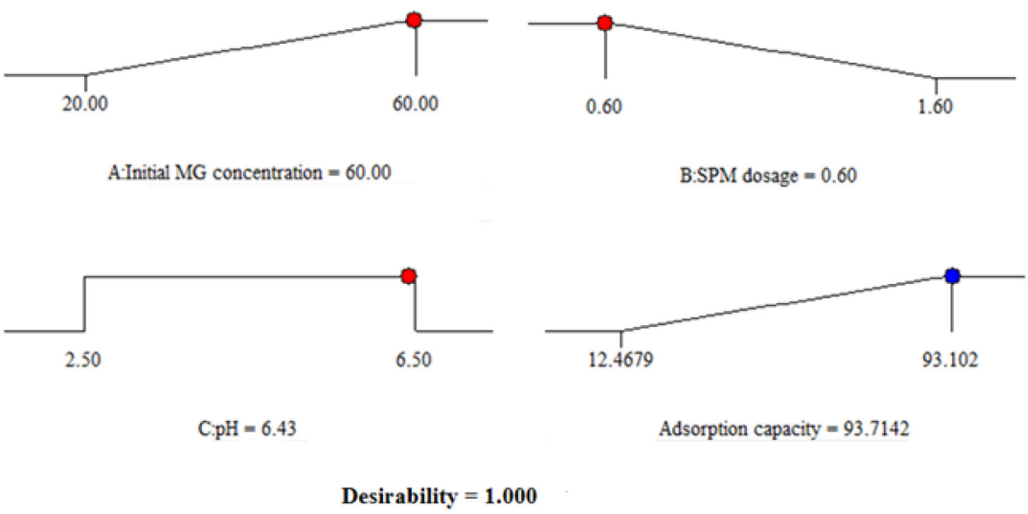

Fig. 10. Desirability ramp for numerical optimization of four goals, namely the initial MG concentration, SPM dosage, pH of solution and adsorption capacity.

3.7. Optimization using the desirability function

Model validation or the experimental confirmation is the final step in the optimization process using response surface model. In the present study for maximum desirability, a minimum level of SPM dosage, maximum level of initial MG concentration, initial solution pH within range of 2.5–6.5 and maximum level of adsorption capacity were set. According the Design Expert software's numerical optimization, desirability is an objective function, which it can normally range from zero to one for any given response. A desirability value of one represents the ideal case. In contrast, a desirability value of zero represents that responses fall outside the desirable limits [50]. Therefore, the predicted optimal conditions for adsorption capacity of MG onto the modified SPM are initial MG concentration of 60 mg L^{-1}, SPM dosage of 0.6 g L^{-1} and pH of solution of 6.43. Under such condition, the adsorption capacity of SPM with desirability of 1.000 is 93.71 mg g^{-1} (Fig. 10).

Finally, to test the validation and accuracy of the predicted adsorption capacity, three additional runs were conducted within the optimized conditions. The actual average adsorption capacity was 94.66 mg g^{-1}. The results indicated that the experimental value closely agreed with the predicted value and the error of the predicted and experimental values was ~1%.

3.8. Regeneration studies

Desorption studies help to elucidate the ability of regeneration and recovery of the adsorbent and adsorbate, respectively. In principle, regeneration ability of the adsorbent after contaminant removal due to economic and resource conservation reasons is an important factor for developing the process. The economic feasibility of using SPM to remove MG from aqueous solution relies on its regeneration ability during multiple adsorption/desorption cycles. To evaluate the possibility of the regeneration and reusability of SPM desorption experiments were performed. The regeneration ratio is defined as the percentage of re-adsorbed to the initial adsorbed MG. In every cycle, for removal of the adsorbed dye ions from the SMP surface, the adsorbent was constantly stirred at methanol solution (1M) as the desorption medium at 160 rpm for 90 min. As observed in Fig 11, the regeneration ratio of SMP was reduced to 35.93% after five cycles, and it may be attributed to the fact that not all the previously adsorbed MG molecules have been desorbed during the regeneration step.

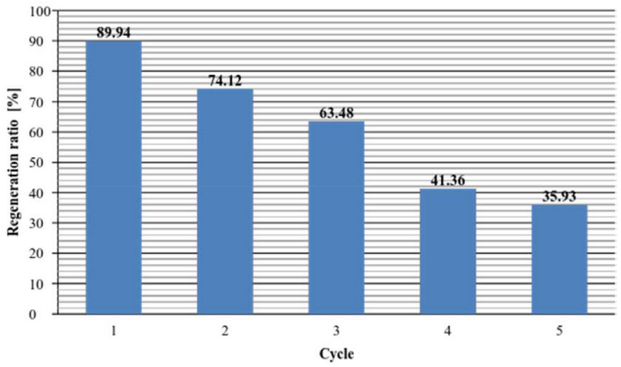

Fig. 11. Regeneration ratio of SPM for MG removal.

4. Conclusions

In the present study, the adsorption capacity of MG onto the acid modified SPM was investigated. For this purpose, Box–Behnken design was used to obtain the optimum level of initial dye concentration, adsorbent dosage, and pH of solution in adsorption process. Second-order regression model was used to describe the effects of factors on the MG uptake. ANOVA results of the regression equation ($p < 0.0001$) indicated that the model was highly significant at 95% of the probability level ($R^2_{adj} = 0.9850$). The results

showed that the effects of the SPM dosage and initial MG concentration were highly significant. At optimum conditions (SPM dosage 0.6 g L^{-1}, initial MG concentration 60 mg L^{-1} and pH 6.43), the predicted adsorption capacity was 93.71 mg g^{-1} and the error of the predicted and experimental values was ~1%.These results indicate that SPM would be used as an alternative and low-cost adsorbent for the removal of MG dye from wastewater. The results of the statistical analysis showed that adsorption of MG onto the modified SPM is well modeled and sorption results are repeatable.

Acknowledgments

The authors would like to thank Iran University of Science & Technology (Iran) for the financial support. The authors would also like to thank Mr. Mostafa Hassani for supplying sphagnum peat moss for this work.

References

[1] S. Kant, D. Pathania, P. Singh, P. Dhiman, A. Kumar, Removal of malachite green and methylene blue by Fe0.01Ni0.01Zn0.98O/polyacrylamide nanocomposite using coupled adsorption and photocatalysis, Appl. Catal. B Environ., 147 (2014) 340–352.

[2] M. Roosta, M. Ghaedi, N. Shokri, A. Daneshfar, R. Sahraei, A. Asghari, Optimization of the combined ultrasonic assisted/adsorption method for the removal of malachite green by gold nanoparticles loaded on activated carbon: experimental design, Spectrochim. Acta. A. Mol. Biomol. Spectrosc., 118 (2014) 55–65.

[3] X. Rong, F. Qiu, J. Qin, J. Yan, H. Zhao, D. Yang, Removal of malachite green from the contaminated water using a water-soluble melamine/maleic anhydride sorbent, J. Ind. Eng. Chem., 20 (2014) 3808–3814.

[4] L. Zhang, H. Zhang, W. Guo, Y. Tian, Removal of malachite green and crystal violet cationic dyes from aqueous solution using activated sintering process red mud, Appl. Clay Sci., 93–94 (2014) 85–93.

[5] Y. Zheng, Y. Zhu, A. Wang, Highly efficient and selective adsorption of malachite green onto granular composite hydrogel, Chem. Eng. J., 257 (2014) 66–73.

[6] M. Ghaedi, and N. Mosallanejad, Study of competitive adsorption of malachite green and sunset yellow dyes on cadmium hydroxide nanowires loaded on activated carbon, J. Ind. Eng. Chem., 20 (2014) 1085–1096.

[7] A. Soni, A. Tiwari, A.K. Bajpai, Removal of malachite green from aqueous solution using nano-iron oxide-loaded alginate microspheres: batch and column studies, Res. Chem. Intermed., 40 (2013) 913–930.

[8] D. Wang, L. Liu, X. Jiang, J. Yu, X. Chen, Adsorption and removal of malachite green from aqueous solution using magnetic β-cyclodextrin-graphene oxide nanocomposites as adsorbents, Colloids Surfaces A Physicochem. Eng. Asp., 466 (2015) 166–173.

[9] Y.C. Lee, E.J. Kim, J.W. Yang, H.J. Shin, Removal of malachite green by adsorption and precipitation using aminopropyl functionalized magnesium phyllosilicate, J. Hazard. Mater., 192 (2011) 62–70.

[10] A. Appusamy, I. John, K. Ponnusamy, A. Ramalingam, Removal of crystal violet dye from aqueous solution using triton X-114 surfactant via cloud point extraction, Eng. Sci. Technol. an Int. J., 17 (2014) 137–144.

[11] J. Chen, J. Mao, X. Mo, J. Hang, M. Yang, Study of adsorption behavior of malachite green on polyethylene glycol micelles in cloud point extraction procedure, Colloids Surfaces A Physicochem. Eng. Asp., 345 (2009) 231–236.

[12] A. Saeed, M. Sharif, M. Iqbal, Application potential of grapefruit peel as dye sorbent: kinetics, equilibrium and mechanism of crystal violet adsorption, J. Hazard. Mater., 179 (2010) 564–572.

[13] H. Ouni, M. Dhahbi, Spectrometric study of crystal violet in presence of polyacrylic acid and polyethylenimine and its removal by polyelectrolyte enhanced ultrafiltration, Sep. Purif. Technol., 72 (2010) 340–346.

[14] D. Morshedi, Z. Mohammadi, M.M. Akbar Boojar, F. Aliakbari, Using protein nanofibrils to remove azo dyes from aqueous solution by the coagulation process, Colloids Surf. B. Biointerfaces, 112 (2013) 245–254.

[15] Z. Yang, H. Yang, Z. Jiang, T. Cai, H. Li, H. Li, A. Li, R. Cheng, Flocculation of both anionic and cationic dyes in aqueous solutions by the amphoteric grafting flocculant carboxymethyl chitosan-graft-polyacrylamide, J. Hazard. Mater., 254–255 (2013) 36–45.

[16] H.I. Chieng, T. Zehra, L.B.L. Lim, N. Priyantha, D.T.B. Tennakoon, Sorption characteristics of peat of Brunei Darussalam IV: equilibrium, thermodynamics and kinetics of adsorption of methylene blue and malachite green dyes from aqueous solution, Environ. Earth Sci., 72 (2014) 2263–2277.

[17] R. Ahmad, I. Hasan, L-cystein modified bentonite-cellulose nanocomposite (cellu/cys-bent) for adsorption of Cu^{2+}, Pb^{2+} and Cd^{2+} ions from aqueous solution, Sep. Sci. Technol., 51 (2016) 381–394.

[18] A. Mittal, R. Ahmad, I. Hasan, Biosorption of Pb^{2+}, Ni^{2+} and Cu^{2+} ions from aqueous solutions by L-cystein-modified montmorillonite-immobilized alginate nanocomposite, Desalin. Water Treat. (in press) 1–18. Available from < http://www.tandfonline.com/doi/abs/10.1080/19443994.2015.1086900 >.

[19] A. Mittal, R. Ahmad, I. Hasan, Poly (methyl methacrylate)-grafted alginate/Fe_3O_4 nanocomposite: synthesis and its application for the removal of heavy metal ions, Desalin. Water Treat., (in press) 1–14. Available from < http://www.tandfonline.com/doi/abs/10.1080/19443994.2015.1104726 >.

[20] A. Mittal, R. Ahmad, I. Hasan, Iron oxide-impregnated dextrin nanocomposite: synthesis and its application for the biosorption of Cr (VI) ions from aqueous solution, Desalin. Water Treat., 57 (2016) 15133–15145.

[21] H. Shayesteh, A. Rahbar-Kelishami, R. Norouzbeigi, Adsorption of malachite green and crystal violet cationic dyes from aqueous solution using pumice stone as a low-cost adsorbent: Kinetic, equilibrium and thermodynamic studies, Desalin. Water Treat., 57 (2016) 12822–12831.

[22] S.D. Khattri, M.K. Singh, Removal of malachite green from dye wastewater using neem sawdust by adsorption, J. Hazard. Mater., 167 (2009) 1089–1094.

[23] R. Han, Y. Wang, Q. Sun, L. Wang, J. Song, X. He, C. Dou, Malachite green adsorption onto natural zeolite and reuse by microwave irradiation, J. Hazard. Mater., 175 (2010) 1056–1061.

[24] A. Wei, B. Liu, H. Zhao, Y. Chen, W. Wang, Y. Ma, H. Yang, S. Liu, Synthesis and formation mechanism of flowerlike architectures assembled from ultrathin NiO nanoflakes and their adsorption to malachite green and acid red in water, Chem. Eng. J., 239 (2014) 141–148.

[25] M.K. Dahri, M.R.R. Kooh, L.B.L. Lim, Water remediation using low cost adsorbent walnut shell for removal of malachite green: Equilibrium, kinetics, thermodynamic and regeneration studies, J. Environ. Chem. Eng., 2 (2014) 1434–1444.

[26] A.A. Jalil, S. Triwahyono, M.R. Yaakob, Z.Z. Azmi, N. Sapawe, N.H. Kamarudin, H.D. Setiabudi, N.F. Jaafar, S.M. Sidik, S.H. Adam, B.H. Hameed, Utilization of bivalve shell-treated Zea mays L. (maize) husk leaf as a low-cost biosorbent for enhanced adsorption of malachite green, Bioresour. Technol., 120 (2012) 218–224.

[27] M.T. Yagub, T.K. Sen, S. Afroze, H.M. Ang, Dye and its removal from aqueous solution by adsorption: a review, Adv. Colloid. Interface Sci., 209 (2014) 172–184.

[28] A.N. Fernandes, C.A. Almeida, C.T. Menezes, N.A. Debacher, M.M. Sierra, Removal of methylene blue from aqueous solution by peat, J. Hazard. Mater., 144 (2007) 412–419.

[29] J.M. Marquez-Reyes, U.J. Lopez-Chuken, A. Valdez-Gonzalez, H.A. Luna-Olvera, Removal of chromium and lead by a sulfate-reducing consortium using peat moss as carbon source, Bioresour. Technol., 144 (2013) 128–134.
[30] E. Lourie, and E. Gjengedal, Metal sorption by peat and algae treated peat: kinetics and factors affecting the process, Chemosphere, 85 (2011) 759–764.
[31] M.P. Koivula, K. Kujala, H. Ronkkomaki, M. Makela, Sorption of Pb(II), Cr(III), Cu(II), As(III) to peat, and utilization of the sorption properties in industrial waste landfill hydraulic barrier layers, J. Hazard. Mater., 164 (2009) 345–352.
[32] V.K. Gupta, and Suhas, Application of low-cost adsorbents for dye removal-a review, J. Environ. Manage., 90 (2009) 2313–2342.
[33] P. Fine, A. Scagnossi, Y. Chen, U. Mingelgrin, Practical and mechanistic aspects of the removal of cadmium from aqueous systems using peat, Environ. Pollut., 138 (2005) 358–367.
[34] A. Srinivasan, T. Viraraghavan, Decolorization of dye wastewaters by biosorbents: a review, J. Environ. Manage., 91 (2010) 1915–1929.
[35] D. Bingöl, S. Veli, S. Zor, U. Özdemir, Analysis of adsorption of reactive azo dye onto $CuCl_2$ doped polyaniline using Box–Behnken design approach, Synth. Met., 162 (2012) 1566–1571.
[36] M. Mourabet, A. El Rhilassi, H. El Boujaady, M. Bennani-Ziatni, R. El Hamri, A. Taitai, Removal of fluoride from aqueous solution by adsorption on Apatitic tricalcium phosphate using Box–Behnken design and desirability function, Appl. Surf. Sci., 258 (2012) 4402–4410.
[37] S. Ray, J.A. Lalman, N. Biswas, Using the Box-Benkhen technique to statistically model phenol photocatalytic degradation by titanium dioxide nanoparticles, Chem. Eng. J., 150 (2009) 15–24.
[38] J. Zolgharnein, A. Shahmoradi, J.B. Ghasemi, Comparative study of Box-Behnken, central composite, and Doehlert matrix for multivariate optimization of Pb (II) adsorption onto Robiniatree leaves, J. Chemom., 27 (2013) 12–20.
[39] S. Chowdhury, R. Mishra, P. Saha, P. Kushwaha, Adsorption thermodynamics, kinetics and isosteric heat of adsorption of malachite green onto chemically modified rice husk, Desalination, 265 (2011) 159–168.
[40] K. Wantala, E. Khongkasem, N. Khlongkarnpanich, S. Sthiannopkao, K.-W. Kim, Optimization of As(V) adsorption on Fe-RH-MCM-41-immobilized GAC using Box–Behnken Design: Effects of pH, loadings, and initial concentrations, Appl. Geochemistry, 27 (2012) 1027–1034.
[41] P. Tripathi, V.C. Srivastava, A. Kumar, Optimization of an azo dye batch adsorption parameters using Box–Behnken design, Desalination, 249 (2009) 1273–1279.
[42] A. Leon-Torres, E.M. Cuerda-Correa, C. Fernandez-Gonzalez, M.F. Alexandre Franco, V. Gomez-Serrano, On the use of a natural peat for the removal of Cr(VI) from aqueous solutions, J. Colloid. Interface. Sci., 386 (2012) 325–332.
[43] S.J. Lee, J. Park, Y.T. Ahn, J. Chung, Comparison of heavy metal adsorption by peat moss and peat moss-derived biochar produced under different carbonization conditions, Water. Air. Soil. Pollut., 226 (2015) 1–11.
[44] T. Aysu, and M.M. Küçük, Removal of crystal violet and methylene blue from aqueous solutions by activated carbon prepared from Ferula orientalis, Int. J. Environ. Sci. Technol., 12 (2014) 2273–2284.
[45] M.A. Ahmad, N. Ahmad, O.S. Bello, Adsorptive removal of malachite green dye using durian seed-based activated carbon, Water. Air. Soil. Pollut., 225 (2014) 1–18.
[46] H. Shayesteh, A. Rahbar-Kelishami, R. Norouzbeigi, Evaluation of natural and cationic surfactant modified pumice for congo red removal in batch mode: Kinetic, equilibrium, and thermodynamic studies, J. Mol. Liq., 221 (2016) 1–11.
[47] M.N. Sepehr, A. Amrane, K.A. Karimaian, M. Zarrabi, H.R. Ghaffari, Potential of waste pumice and surface modified pumice for hexavalent chromium removal: Characterization, equilibrium, thermodynamic and kinetic study, J. Taiwan Inst. Chem. Eng., 45 (2014) 635–647.
[48] Q. Ma, L. Wang, Adsorption of Reactive blue 21 onto functionalized cellulose under ultrasonic pretreatment: Kinetic and equilibrium study, J. Taiwan Inst. Chem. Eng., 50 (2015) 229–235.
[49] M. Kıranşan, R.D.C. Soltani, A. Hassani, S. Karaca, A. Khataee, Preparation of cetyltrimethylammonium bromide modified montmorillonite nanomaterial for adsorption of a textile dye, J. Taiwan Inst. Chem. Eng., 45 (2014) 2565–2577.
[50] S. Chowdhury, S. Chakraborty, P.D. Saha, Response surface optimization of a dynamic dye adsorption process: a case study of crystal violet adsorption onto NaOH-modified rice husk, Environ. sci. pollut. res. int., 20 (2013) 1698–1705.
[51] Z. Zhang, Q. Pang, M. Li, H. Zheng, H. Chen, K. Chen, Optimization of the condition for adsorption of gallic acid by Aspergillus oryzae mycelia using Box-Behnken design, Environ. sci. pollut. res. int l, 22 (2015) 1085–1094.
[52] E. Alemayehu, B. Lennartz, Adsorptive removal of nickel from water using volcanic rocks, Appl. Geochemistry, 25 (2010) 1596–1602.
[53] S. Neupane, S.T. Ramesh, R. Gandhimathi, P.V. Nidheesh, Pineapple leaf (Ananas comosus) powder as a biosorbent for the removal of crystal violet from aqueous solution, Desalin. Water Treat., 54 (2014) 2041–2054.